

A comparison of GRACE-derived temporal gravity variations with observations of six European superconducting gravimeters

M. Abe,¹ C. Kroner,² C. Förste,¹ S. Petrovic,¹ F. Barthelmes,¹ A. Weise,³ A. Güntner,¹ B. Creutzfeldt,¹ T. Jahr,³ G. Jentzsch,³ H. Wilmes⁴ and H. Wziontek⁴

¹Helmholtz Centre Potsdam, German Research Centre for Geosciences GFZ, Telegrafenberg, D-14473 Potsdam, Germany. E-mail: abe@gfz-potsdam.de

²Physikalisch-Technische Bundesanstalt PTB, Bundesallee 100, D-38116 Braunschweig, Germany

³Institute of Geosciences, Applied Geophysics, Friedrich-Schiller-University, Burgweg 11, D-07749 Jena, Germany

⁴Federal Agency for Cartography and Geodesy (BKG), Richard-Strauss-Allee 11, D-60598 Frankfurt/M., Germany

Accepted 2012 August 2. Received 2012 August 2; in original form 2010 November 18

SUMMARY

The GRACE (Gravity Recovery and Climate Experiment) satellite mission provides global time-series of the Earth's gravity field. In view of limited resolution and noise from the GRACE data, various filtering techniques have been developed to extract an optimal signal. There is no conclusion on the best filter method so far, however. On the other hand, terrestrial gravity observations from superconducting gravimeters (SGs) provide variations of the gravity field with very high accuracy and time resolution, but only at single points. The aim of this study is to compare GRACE-derived temporal gravity variations with gravity time-series within a network of six Central European SG stations. Empirical orthogonal functions (EOF) analysis was applied to detect common signal characteristics over a 3 yr period (2004–2006). rms Differences between the time-series of several GRACE solutions amount to 60 per cent of the rms variability of the individual data sets. The rms differences between the SG and GRACE time-series are about 70 per cent of the rms value of the SG observations. The best agreement between SG and GRACE is obtained when using a Gaussian filter with filter lengths of 800–1250 km for the GRACE data. With the EOF analysis, a common regional signal can be deduced from all gravity data sets. Nevertheless, differences in the first EOF among the GRACE solutions were up to 40 per cent, and differences of up to 50 per cent were found between the SG-based terrestrial and the GRACE-based satellite observations.

Key words: Time-series analysis; Numerical solutions; Satellite geodesy; Time variable gravity; Satellite gravity; Europe.

1 INTRODUCTION

Observation of time-variable gravity is of increasing significance to geosciences such as geophysics and climate research. In particular two kinds of time-variable gravity data with opposing spatial characteristics are important: the global time-variable GRACE (Gravity Recovery and Climate Experiment) gravity field models and the locally recorded gravity time-series of superconducting gravity meters.

The GRACE satellite mission (Tapley & Reigber 2001) is a joint NASA (National Aeronautics and Space Administration) and DLR (Deutsches Zentrum für Luft- und Raumfahrt) project. This gravity satellite mission has been running since 2002 March. Meanwhile 10 yr of GRACE data are available. The GRACE mission provides global estimates of the mean and time-variable gravity field of the Earth. The time-variable GRACE gravity field solutions are particularly useful for detecting mass redistributions on the Earth's surface, such as ice melting in Greenland, Antarctica and Alaska

(e.g. Luthcke *et al.* 2006a; Velicogna & Wahr 2006; Tamisiea *et al.* 2007). To reveal such results with sufficient reliability, however, it is necessary to suppress the noise of the GRACE gravity field solutions. This noise reduction is typically achieved by smoothing the individual GRACE gravity field solutions in the spatial domain using post-processing filter techniques. Discussions on the best filter algorithms to detect mass variations (e.g. continental water storage variations) in the temporal gravity field variations are still ongoing, however, and we offer our study as a contribution to this discussion.

The overall accuracy of the time-variable GRACE gravity field series is roughly a few micro-Gal (10^{-6} Gal = 10^{-8} m s⁻²). Since superconducting gravimetry observations have a reliable long-term stability and since they are also of μ Gal accuracy, it makes sense to compare the GRACE-based gravity variations locally with superconducting gravity recordings. Furthermore, such a comparison should be capable of investigating the effect of the filter techniques applied on the GRACE data. In this context Crossley & Hinderer (2002) introduced the idea that the superconducting gravimeter

(SG) network in Europe may provide a kind of ground truth for the GRACE satellite mission. In their study, they used 190 d of SG data (1997 July to 1998 January, sampling rate 1 hr) from eight European stations and they found a high correlation between the time-series of these six stations. Hinderer *et al.* (2006) and Neumeyer *et al.* (2006b) compared seasonal gravity changes derived from GRACE, with global hydrological models and SGs measurements. They found quite a good agreement within these time-series. Crossley *et al.* (2004, 2009), Neumeyer *et al.* (2008) and Weise *et al.* (2011) applied empirical orthogonal functions (EOF) to detect dominant signals in the satellite-derived time-series and the terrestrial gravity data.

One important difference between these mentioned studies is that Crossley *et al.*, in 2004 and in 2009, used a spatial interpolation algorithm for the terrestrial gravity data sets, before applying the EOF analyses, while Neumeyer *et al.* (2008) and Weise *et al.* (2011) introduced the terrestrial data directly into the EOF analyses

Our own study is based on the studies by Neumeyer *et al.* (2008) and Weise *et al.* (2011) and performs a continuation and widening of the investigations of these authors. Now, not only are the GRACE solutions from GFZ included, but also the CSR and JPL time-series, in comparisons with the SG data. Furthermore additional filters have been applied.

In our study we applied two different kinds of analyses to both data types: (1) To get a first indication of the agreement between the data sets, simple comparisons of correlation coefficients and rms values, for monthly data sets and for the time-series of differences between the SG and the GRACE time-series. (2) To compare the spatial and temporal characteristics of the time-series between these data, the EOF approach has been applied.

2 DATA

2.1 Superconducting gravimetry data

The SG is the most sensitive gravimeter presently available for the continuous monitoring of temporal variations in the Earth's gravity field. Its time-domain accuracy for long periods can be estimated as 0.1 μGal (Hinderer *et al.* 2007). It is a relative gravimeter and has a stable drift rate of typically a few micro-Gal per year. To verify the stability of the calibration factor and to ensure the long-term reliability of the data, the observations need to be verified with repeated absolute gravimeter (AG) measurements. Presently, there are about 30 SG stations worldwide. These stations constitute the so-called Global Geodynamics Project (GGP) network (Crossley *et al.* 1999), which began in 1997. Among others, the objectives of this project are (1) to detect the Earth's core modes, which would provide information about the geodynamo, (2) to study long-term phenomena, such as polar motion and postglacial rebound and (3) to investigate mass redistribution phenomena.

The area of central Europe where 10 SG stations with long-term observations are located is well suited to our study, due to the closely distributed sites with distances between 225 and 880 km. This is a good precondition for the comparison of terrestrial gravity observations with satellite-derived gravity variations. Six SG stations, Bad Homburg (BH) in Germany, Medicina (MC) in Italy, Moxa (MO) in Germany, Strasbourg (ST) in France, Vienna (VI) in Austria and Wetzell (WE) in Germany, have been chosen for this study because of the good quality of their data and the long-term and stable observations. The location of these six SG stations is given in Fig. 1. The time period from 2004 January to 2006 December was chosen for

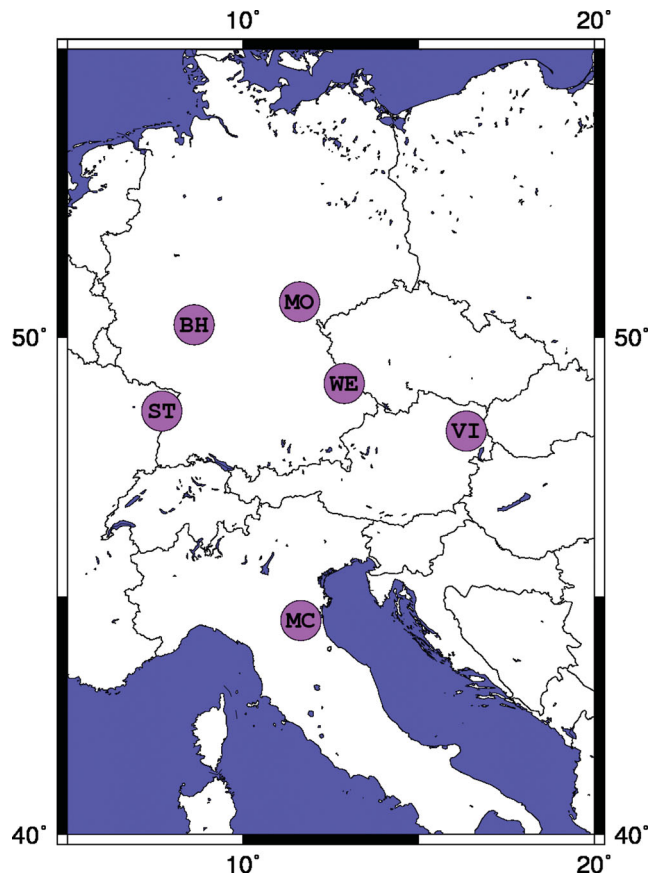


Figure 1. Location of superconducting gravimeter stations in central Europe as used in this study: Bad Homburg (BH), Medicina (MC), Moxa (MO), Strasbourg (ST), Vienna (VI) and Wetzell (WE).

this study, since the data from all six stations were available only for this period.

Typically, raw SG data have a sampling rate of 1 s. The GGP database provides a time-series with a sample rate of 1 min. These data are filtered and decimated by the site operators without applying any corrections (repair-code 00). During the pre-processing, spikes, steps, larger disturbances, for example, related to large earthquakes or maintenance work, were eliminated and the short gaps were filled with model values. Data with higher temporal resolution of 5 resp. 10 s were used instead of GGP data to improve the quality of the pre-processing to reduce tidal effects almost completely from the gravity time-series, a tidal analysis was performed for each station. After restoring the preliminary tidal model, which was applied during the pre-processing steps, effects caused by atmosphere and ocean loading were reduced using the models listed in Table 1. Then a set of tidal frequencies (Tamura 1987) up to periods of 29 d was analysed (Wenzel 1996) for each station. Long periodic tides were added later based on the theoretical model of Dehant *et al.* (1999). The tidal model was then applied and the temporal resolution of the time-series was further reduced to a 1 hr sampling rate using appropriate anti-alias filters. Finally, the effect of polar motion was eliminated. In Table 1 all models are listed. With this process comparability with the GRACE-based gravity variations is ensured, taking the different impacts of the individual gravity effects on terrestrial- and space-born observations into account.

The terrestrial gravity observations are very sensitive to local mass redistributions mainly from local hydrological variations. Typically most of the effect originates from a zone of about 250 m

Table 1. Reductions applied to the terrestrial gravity time-series.

Reductions	Model
Solid earth tides	Local analysis (see text)
Ocean tide loading	FES 2004 (Lyard <i>et al.</i> 2006)
Atmosphere	Newtonian attraction and deformation based on 3D atmospheric data: Moxa (MO), Strasbourg (ST) and Vienna (VI): European Center for Medium-Range Weather Forecasts (ECMWF), Neumeyer <i>et al.</i> (2004, 2006a), Abe <i>et al.</i> (2010). Bad Homburg (BH), Medicina (MC) and Wetzell (WE): German Weather Service (DWD), Klügel & Wziontek (2009)
Polar motion and	Based on Wahr (1985) using a delta factor of 1.16 the pole coordinates (EOP C04 series) provided by the International Earth Rotation Service (IERS).

around the gravimeter in a hilly area (e.g. Hokkanen *et al.* 2006; Weise *et al.* 2009; Creutzfeldt *et al.* 2010a,b). Models were applied to evidently affected stations (MO, ST, VI and WE), to eliminate local hydrological effects from the SG time-series, MO, ST and VI are “subsurface” stations, where local mass variations occur above and below the gravity sensor. For the MO station, a 3-D hydrological model was developed and used (Naujoks *et al.* 2010). The included area is $2 \times 2 \text{ km}^2$ and soil water storage, groundwater storage, snow storage and interception storage were used for the computation. The local hydrological effect at ST was estimated by using precipitation data and the consideration of evapotranspiration for a computation area of $40 \times 50 \text{ m}^2$. For the VI station, hourly precipitation, snow depth, air temperature and global radiation data were used, as provided by the Central Institute for Meteorology and Geodynamics (ZAMG). The incorporated area has a diameter of 1 km. The local hydrological model for the WE station has been developed by Creutzfeldt *et al.* (2010a,b). Water storage changes were calculated using soil moisture measurements and groundwater level variations. An area of $4 \times 4 \text{ km}^2$ around the station was included in the modelling, considering the spatial distribution of mass changes along the topography (Creutzfeldt *et al.* 2008).

For the stations at BH and MC, local hydrological corrections were not applied because no significant local effects were expected at either location. Station BH is situated in a mainly sealed urban area on a rock. A very low pore volume of the bedrock with almost no fissures, in conjunction with the well-drained or sealed surrounding area, might cause only small water storage changes within the radius of influence for local attraction effects. Station MC is located in the Po river plain with intensive agricultural use in its vicinity. It can be assumed that irrigation and drainage of the neighbouring farmland alters or compensates for largely natural changes in the local water storage. The residual gravity time-series at both stations show mainly seasonal variations not exceeding $3 \mu\text{Gal}$ in amplitude. This agrees well with attraction and deformation effects computed from global hydrological models (Wziontek *et al.* 2009).

After the mentioned pre-processing steps and reductions, the obtained gravity residuals were averaged to monthly values, making them comparable with the GRACE time-series. It should be noted, that a significant outlier in the obtained SG monthly time-series of WE in 2005 January was removed and interpolated beforehand.

2.2 GRACE gravity time-series

GRACE products are routinely generated by three different institutions of the GRACE Science Data System (SDS): (1) the Cen-

ter for Space Research (CSR) at the University of Austin/Texas (Bettadpur 2007), (2) the GFZ German Research Centre for Geosciences in Germany (Flechtner 2007) and (3) the Jet Propulsion Laboratory (JPL) in Pasadena/California (Watkins & Yuan 2007). The main GRACE time-variable gravity products provided by these three processing centres are time-series of monthly global gravity field models given in terms of spherical harmonic coefficients. The Groupe de Recherches de Géodésie Spatiale (GRGS) at the French Centre National d'Etudes Spatiales (CNES) in Toulouse/France also provides monthly GRACE gravity field models. GRGS/CNES produces GRACE gravity field time-series of a temporal resolution of 10 d as well (Lemoine *et al.* 2007; Bruinsma *et al.* 2009). The highest temporal resolutions of the presently published GRACE gravity field time-series have the daily solutions from the Bonn University (Kurtenbach *et al.* 2009) and the 7 d solutions from GFZ (Flechtner *et al.* 2010).

In this study we included the monthly GRACE gravity time-series from the three SDS institutions; that means we used the three independently generated Release 4 GRACE Level-2 products from GFZ (Flechtner 2007), CSR (Bettadpur 2007) and JPL (Watkins & Yuan 2007). The maximum degree/order of the GFZ and JPL monthly solutions is 120, but it is only 60 for the CSR solutions. All these data sets from 2002 April onwards are available to download from the GFZ Information System and Data Center (ISDC, <http://isdc.gfz-potsdam.de/>) and from the International Centre for Global Earth Models (ICGEM, <http://icgem.gfz-potsdam.de/ICGEM/>), both at GFZ Potsdam. The monthly solution for 2003 June is not available for CSR and JPL solutions and the data sets for 2003 January and June and 2004 January are not available in the GFZ solutions.

To filter the monthly gravity field models in the spatial domain, various filter types have been developed for this purpose. An isotropic Gaussian filter that is used widely nowadays was proposed by Wahr *et al.* (1998) and is based on an algorithm of Jekeli (1981). Kusche (2007) and Kusche *et al.* (2009) developed a non-isotropic filter using a decorrelation algorithm. Han *et al.* (2005) found that using a non-isotropic filter rather than an isotropic one yields a higher spatial resolution, and improves the correlation of the smoothed GRACE-derived signal with geophysical models (e.g. hydrological model, ocean circulation model).

In this study, two types of filter were considered. One is an isotropic Gaussian filter. We used radii of 330, 400, 500, 660, 800, 1000, 1250 and 1600 km for the Gaussian filter length, and an optimal radius was determined from the point of view of the terrestrial gravity observations. The other filter is the non-isotropic one presented by Kusche (2007) and Kusche *et al.* (2009). This filter reduces the north–south error structure in the GRACE solutions much more than the Gaussian filter (Kusche 2007). We have used three different smoothing factors of $a = 1 \times 10^{14}$ (DDK1), $a = 1 \times 10^{13}$ (DDK2) and $a = 1 \times 10^{12}$ (DDK3) in the eq. (22) ($\bar{x}_{\gamma(a)} = (\bar{N} + a\bar{M})^{-1}\bar{N}\hat{x} = \bar{W}_{\gamma(a)}\hat{x}$) in Kusche (2007), and DDK1 is the strongest filter among them.

To compare the terrestrial SG observations with the satellite-derived variations, it is necessary to take into account the height-induced loading effect that is additionally contained in the SG data. This part has been modelled applying the degree-dependent load Love numbers and Green's functions, and has been added to the GRACE gravity time-series. Detailed explanations on the computation of the loading-induced height effect can be found in Neumeyer *et al.* (2006b, eq. 15, and 2008, eq. 1), which result in the following

expression:

$$\begin{aligned} \delta(\varphi, \lambda) &= \delta g_G + \delta g_{\text{load}} \\ &= \frac{GM}{R^2} \sum_{l=0}^{l_{\text{max}}} (l+1-2h'_l) \\ &\sum_{m=0}^l [\delta \bar{C}_{lm}^G \cos(m\lambda) + \delta \bar{S}_{lm}^G \sin(m\lambda)] \bar{P}_{lm}(\sin \varphi). \end{aligned} \quad (1)$$

In this formula, (φ, λ) are spherical geocentric coordinates (latitude, longitude) of the computation point, R is the mean radius of the Earth, GM is the gravitational constant times mass of the Earth, l , m are the degree and order of the spherical harmonics, l_{max} is the chosen maximum degree for the calculations ($l_{\text{max}} < \infty$) and h'_l is the degree-dependent load Love Number (Farrell 1972).

3 COMPARISON OF TIME VARIABILITY DEDUCED FROM SG AND GRACE

Fig. 2 shows a general comparison of the time-series of SG gravity residuals, the CSR, GFZ and JPL GRACE solutions with Gaussian filter length of 1000 km applied, and a GFZ GRACE solution after

applying the decorrelation filter DDK1, all of them covering a period of 6 yr.

In all these plotted time-series, seasonal variations can be seen with maximum signal in winter/spring and minimum signal at the end of summer. From this general annual comparison, it is found that the time-series of the SG data and the GRACE solutions (from GFZ, CSR and JPL), with two different filters applied, are basically in accordance. Visible differences also exist, however, among the time-series. For instance, the largest discrepancy of about 4 μGal is found at WE station between the time-series of SG and the GFZ and JPL GRACE-derived gravity variations during 2005 January. For evaluation, the overall rms and correlation coefficients have been computed (see Section 3.2).

Additionally, the differences between the GRACE solutions are not negligible. The amplitudes of the GRACE solutions based on the DDK1 filter are slightly larger than for the data based on the Gaussian filter length of 1000 km. The differences between the GFZ and JPL solutions reach around 2 μGal in 2007 January. The systematic discrepancies are not easily seen in detail from Fig. 2, however.

Different GRACE solutions were therefore compared, to estimate the discrepancies between the GRACE solutions at the SG sites (Section 3.1).

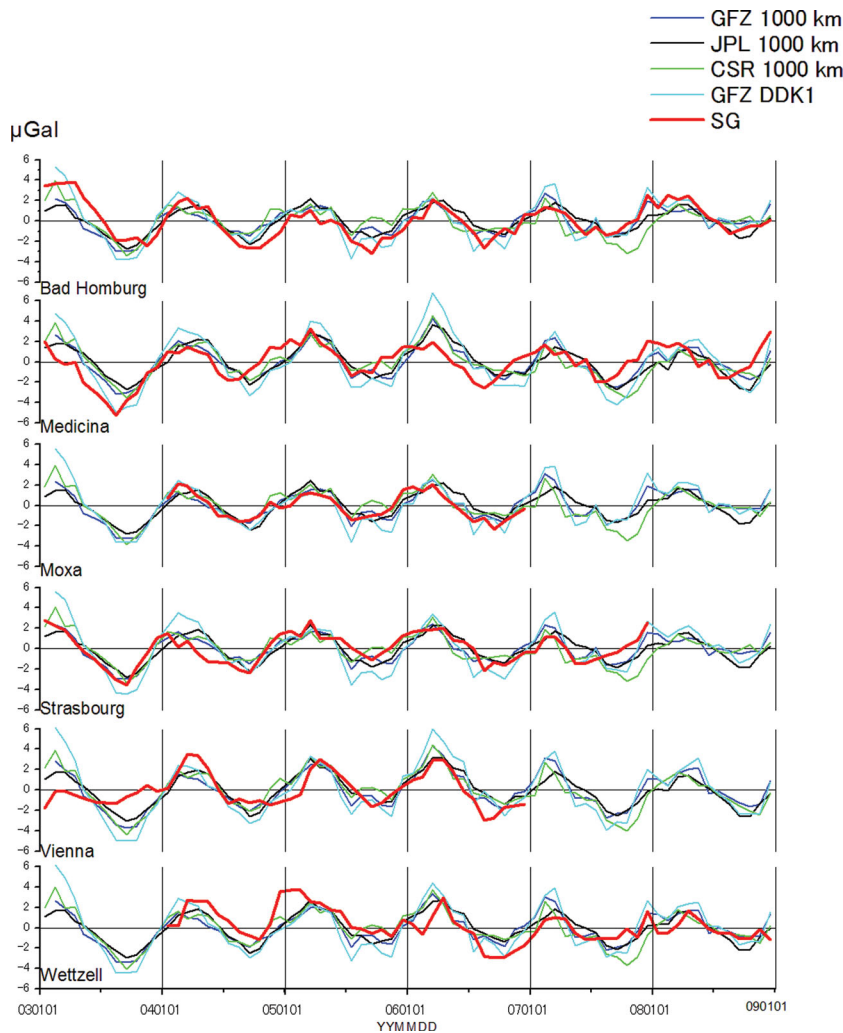


Figure 2. Monthly time-series of SG residuals and GRACE-derived gravity variations (different processing centres, details see text) with a Gaussian filter of 1000 km and a comparable non-isotropic filter applied for six European SG stations from 2003 to 2008.

Table 2. rms of monthly SG- and GRACE-derived gravity variations (μGal) and overall rms values for all stations, for different types of filtering of the satellite data from 2004 to 2006 (for details see text). The shaded values represent the two rms values of the GRACE solutions closest to the rms values of the SG data.

		Bad Homburg rms (μGal)	Medicina rms (μGal)	Moxa rms (μGal)	Strasbourg rms (μGal)	Vienna rms (μGal)	Wetzell rms (μGal)	Overall rms μGal
1	SG	1.30	1.40	1.11	1.30	1.64	1.91	1.47
2	GFZ 1600 km	0.81	0.99	0.91	0.80	1.14	0.99	0.95
3	GFZ 1250 km	0.94	1.27	1.05	0.97	1.37	1.17	1.14
4	GFZ 1000 km	1.07	1.55	1.17	1.15	1.57	1.34	1.32
5	GFZ 800 km	1.24	1.84	1.30	1.38	1.77	1.52	1.52
6	GFZ 660 km	1.45	2.07	1.44	1.65	1.94	1.69	1.72
7	GFZ 500 km	1.99	2.35	1.77	2.26	2.20	1.98	2.10
8	GFZ 400 km	2.81	2.63	2.31	3.10	2.55	2.32	2.63
9	GFZ 330 km	4.01	3.25	3.24	4.27	3.49	2.76	3.54
10	GFZ DDK1	1.66	2.58	1.61	2.02	2.29	2.01	2.06
11	GFZ DDK2	2.41	2.77	2.21	2.93	2.59	2.57	2.59
12	GFZ DDK3	3.39	3.08	3.03	3.92	2.94	3.02	3.25
13	CSR 1600 km	0.85	0.92	0.94	0.83	1.12	0.98	0.95
14	CSR 1250 km	0.95	1.17	1.04	0.95	1.33	1.14	1.10
15	CSR 1000 km	1.05	1.41	1.13	1.09	1.52	1.27	1.26
16	CSR 800 km	1.16	1.68	1.22	1.26	1.71	1.42	1.42
17	CSR 660 km	1.30	1.91	1.33	1.46	1.88	1.59	1.60
18	CSR 500 km	1.70	2.23	1.66	1.94	2.19	1.92	1.95
19	CSR 400 km	2.33	2.57	2.10	2.58	2.61	2.35	2.43
20	CSR 330 km	3.34	3.21	2.73	3.52	3.32	3.16	3.22
21	CSR DDK1	1.48	2.37	1.44	1.80	2.22	1.85	1.89
22	CSR DDK2	1.89	2.40	1.87	2.38	2.51	2.28	2.24
23	CSR DDK3	2.56	2.66	2.75	3.00	2.94	2.87	2.80
24	JPL 1600 km	0.89	1.00	0.93	0.90	1.05	0.99	0.96
25	JPL 1250 km	1.06	1.30	1.11	1.11	1.31	1.21	1.19
26	JPL 1000 km	1.20	1.57	1.25	1.29	1.54	1.39	1.38
27	JPL 800 km	1.34	1.83	1.37	1.48	1.76	1.58	1.57
28	JPL 660 km	1.47	2.04	1.47	1.67	1.94	1.72	1.73
29	JPL 500 km	1.66	2.40	1.59	2.00	2.08	1.87	1.95
30	JPL 400 km	1.90	3.30	1.84	2.32	2.09	2.07	2.31
31	JPL 330 km	2.49	5.52	2.47	2.86	2.51	2.73	3.28
32	JPL DDK1	1.75	2.62	1.71	2.11	2.38	2.10	2.14
33	JPL DDK2	2.28	3.30	2.13	2.69	2.50	2.42	2.58
34	JPL DDK3	4.02	6.70	3.25	4.28	2.84	4.13	4.38

In this further step, the influence of the chosen filter version on the agreement between SG and GRACE was investigated. After choosing the appropriate filter, an investigation ensued into what common signal could exist with respect to the whole of central Europe.

3.1 Comparison between the GRACE-derived gravity variations

To clarify the level of the basic agreement between the GRACE monthly solutions provided by the different processing centres, we calculated the rms values for individual GRACE time-series (Table 2), overall rms values of differences [rms(diff)] and correlation coefficients between corresponding GRACE solutions (Fig. 3).

First of all, rms values for all data sets are calculated. Let

$$X_i = |X_i(t_1), X_i(t_2), \dots, X_i(t_n)|^T = |X_i(t_j)|^T, (j = 1, \dots, n) \quad (2)$$

denote a time-series at the location i ($i = 1, \dots, k$). Taking into account the mean value of the time-series

$$\overline{X_i(t)} = \frac{\sum_{j=1}^n X_i(t_j)}{n}, \quad (3)$$

we denote:

$$x_i = [X_i(t_1) - \overline{X_i(t)}, X_i(t_2) - \overline{X_i(t)}, \dots, X_i(t_n) - \overline{X_i(t)}]^T \quad (4)$$

then, the rms of the time-series X_i is

$$\sigma(X_i) = \sqrt{\frac{x_i^T x_i}{n}}. \quad (5)$$

The overall rms values

$$\sigma(X) = \sqrt{\frac{\sum_{i=1}^k x_i^T x_i}{kn}} \quad (6)$$

are computed using the time-series for all the considered stations.

The correlation between the time-series X_i and Y_i at the station i is

$$r(X_i, Y_i) = \frac{x_i^T y_i}{\sqrt{(x_i^T x_i)(y_i^T y_i)}}. \quad (7)$$

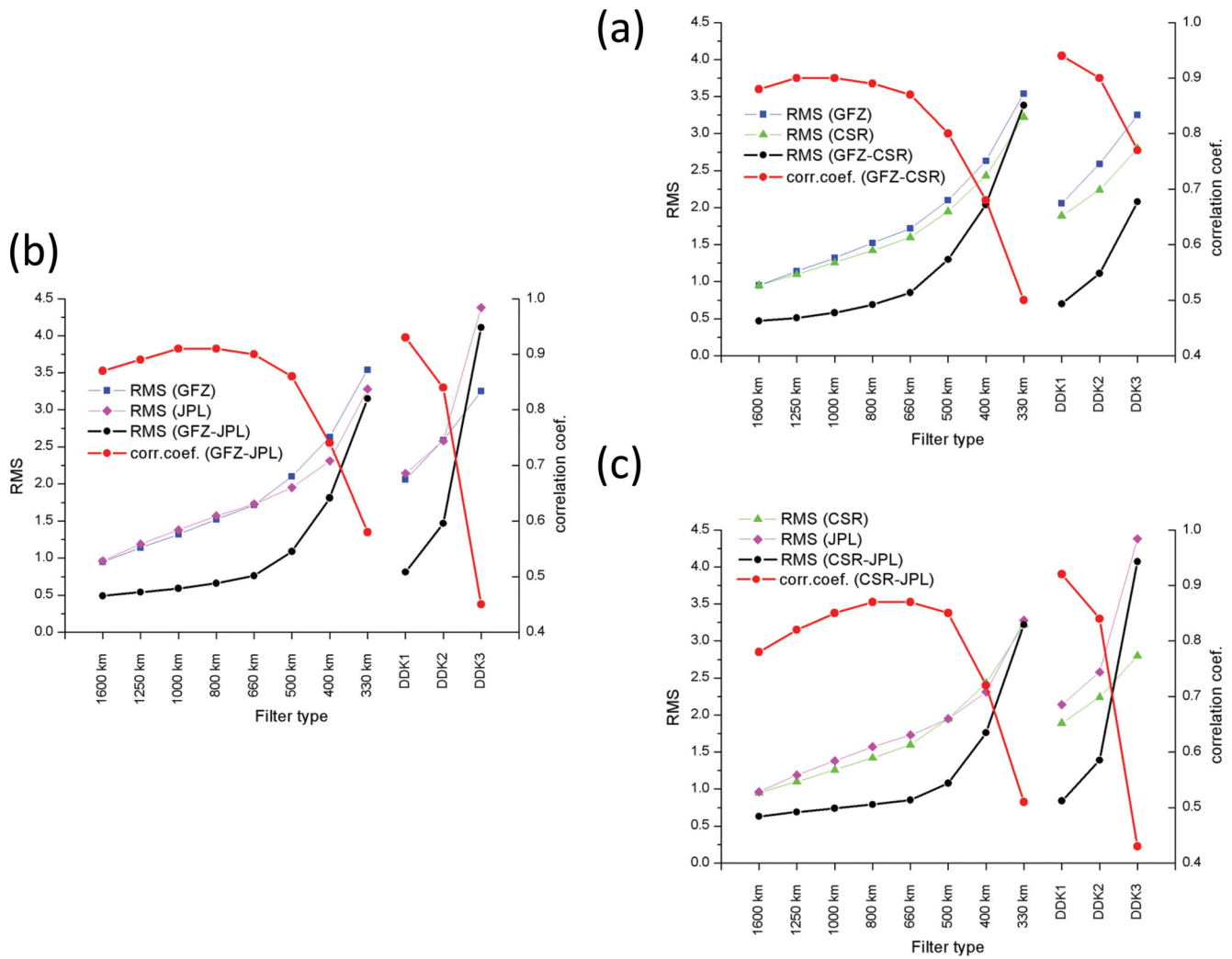


Figure 3. Overall rms values of GRACE-derived gravity variations from two GRACE solutions (μGal), rms of signal differences [rms(diff)] in micro-Gal and overall correlation coefficients between both solutions: (a) GFZ and CSR, (b) GFZ and JPL and (c) CSR and JPL.

The overall correlation is defined by

$$r(X, Y) = \frac{\sum_{i=1}^k x_i^T y_i}{\sqrt{\left(\sum_{i=1}^k x_i^T x_i\right) \left(\sum_{i=1}^k y_i^T y_i\right)}} \quad (8)$$

The rms(diff) between GFZ and CSR, for instance, means that the rms value of difference between the gravity variation derived by GFZ and CSR is computed.

Table 2 shows a comparison of the rms values of the SG residuals and of three different GRACE solutions filtered with de-correlation filters DDK1 to DDK3, and a Gaussian filter of different lengths, for evaluation of the highest agreement with respect to the filter length. Overall rms values for all stations are also shown. From this table, the effect of the different filters, in particular the impact of different filter lengths, can be seen. The filter lengths are related to the smoothing of the time-series. The tendency of the Gaussian filtering is as expected. This means the signal power for all GRACE solutions increases when the filter length is shorter.

The rms value after the application of the most effective de-correlation filter (DDK1) is of the same order of magnitude as for Gaussian filters of filter lengths between 500 and 660 km.

Fig. 3 shows: (1) overall rms values for the time-series of related GRACE-derived gravity variations (column of overall rms in Table 2); (2) rms values of the signal differences [rms(diff)] between two of the respective GFZ, CSR and JPL solutions; and (3) overall correlation coefficients for the monthly time-series.

The rms(diff) values between GFZ and CSR, as well as between GFZ and JPL, show similar variations and similar values, except after applying the DDK3 filter. This discrepancy is caused by the JPL solution after applying the DDK3 filter, because for this solution the overall rms value increases more than twice. The DDK3 filter is so weak in comparison to the other filters, that such different variations are imaginable. The rms(diff) between CSR and JPL are slightly larger than those between GFZ and CSR or GFZ and JPL. The rms(diff) applied to the time-series filtered by a Gaussian filter of lengths between 660 and 1600 km and with the DDK1 filter, accounts for around 50 per cent of the overall rms values of the original monthly GRACE gravity variations.

The overall correlation coefficients between GFZ and CSR vary between 0.50 and 0.94 while those between GFZ and JPL are in the range of 0.45–0.93. CSR and JPL overall correlation coefficients vary between 0.43 and 0.92. It is clearly seen, when the DDK3 filter is used, that the overall correlation coefficients have the lowest values, and when Gaussian filters of medium lengths (between 660

and 1600 km) are applied to the GRACE solutions, these values are relatively high.

The rms(diff) between GRACE solutions reaches almost 60 per cent of the individual signals (including noise), although the source of the original signal is the same. Thus we assume that differences in the data processing at the different GRACE processing centres (e.g. the estimation techniques used at each centre, differences in the modelling of satellite tracks, different treatment of numerical problems or differences in the background environmental modelling) should be responsible for these discrepancies.

This fact should be also taken into account when comparing the temporal variations between GRACE solutions and the SG data in the next section.

3.2 Comparison between the SG- and GRACE-derived gravity variations

First, the rms values of monthly SG- and GRACE-derived gravity variations have been compared (Table 2). The closest rms values between both data sets are found for a Gaussian filter length between 1250 and 660 km, except for the WE station. This is because the SG data at WE have the largest rms value among all the SG stations. This value (1.91 μGal) is nearly double the value at MO (1.11 μGal , Table 2). In the work of Neumeyer *et al.* (2008), the same tendency was found. The rms value for SG in WE was 2.35 and for MO 0.87. For the GRACE solutions, however, such a discrepancy between WE and MO is not found, either in this or in the above-mentioned previous study.

The next investigation looked at which kind of filter and filter parameter, when applied to the GRACE solutions, resulted in the highest agreement between satellite and SG data. In Fig. 4, overall rms (μGal) values of differences [rms(diff)] and correlation coefficients between SG residuals and corresponding GRACE solutions are considered.

Fig. 4 shows that the lowest rms(diff) values between the SG and the GRACE data are found generally for Gaussian filter lengths between 800 and 1600 km. In this range, these rms(diff) values amount to 70–80 per cent of the rms values of the SG time-series. However, it should be taken into account that the discrepancies between GRACE solutions account for around 60 per cent of the original GRACE-derived gravity variations.

The correlation coefficients between the SG and GRACE solutions vary between 0.67 and 0.72 in the range of Gaussian filter lengths between 800 and 1600 km. The overall correlation coefficients of JPL for this filter range are slightly higher than for the other two solutions.

The results for Gaussian filter lengths between 800 and 1600 km are in good agreement with SG data.

The GRACE time-series smoothed with a Gaussian filter of 330 or 400 km length, or with a DDK3 filter, show smaller overall correlation coefficients and larger overall rms(diff) values than those with Gaussian filters of medium length. The reason for this is that the GRACE solutions filtered with a Gaussian filter length of 330 km, 400 km or filter DDK3 still contain considerable errors (stripes-noise) within the high-frequency signals, represented by the higher degree spherical harmonics of the GRACE solutions.

In Neumeyer *et al.* (2008), the correlation coefficient of 0.77 between the SG time-series and the GRACE solution for WE station was calculated by using GFZ solutions with a Gaussian filter length of 660 km. In this study, a value of 0.65 was obtained. A test calculation showed that the different time periods were not the main reason for this discrepancy.

Hence, the differences are probably caused by different corrections for local hydrology used in the two studies. Neumeyer *et al.* (2008) applied a simple regression based on groundwater level variations and concluded that a local hydrological model based on total water storage changes should be developed. Accordingly, an extended local hydrological model by Creutzfeldt *et al.* (2010a,b)

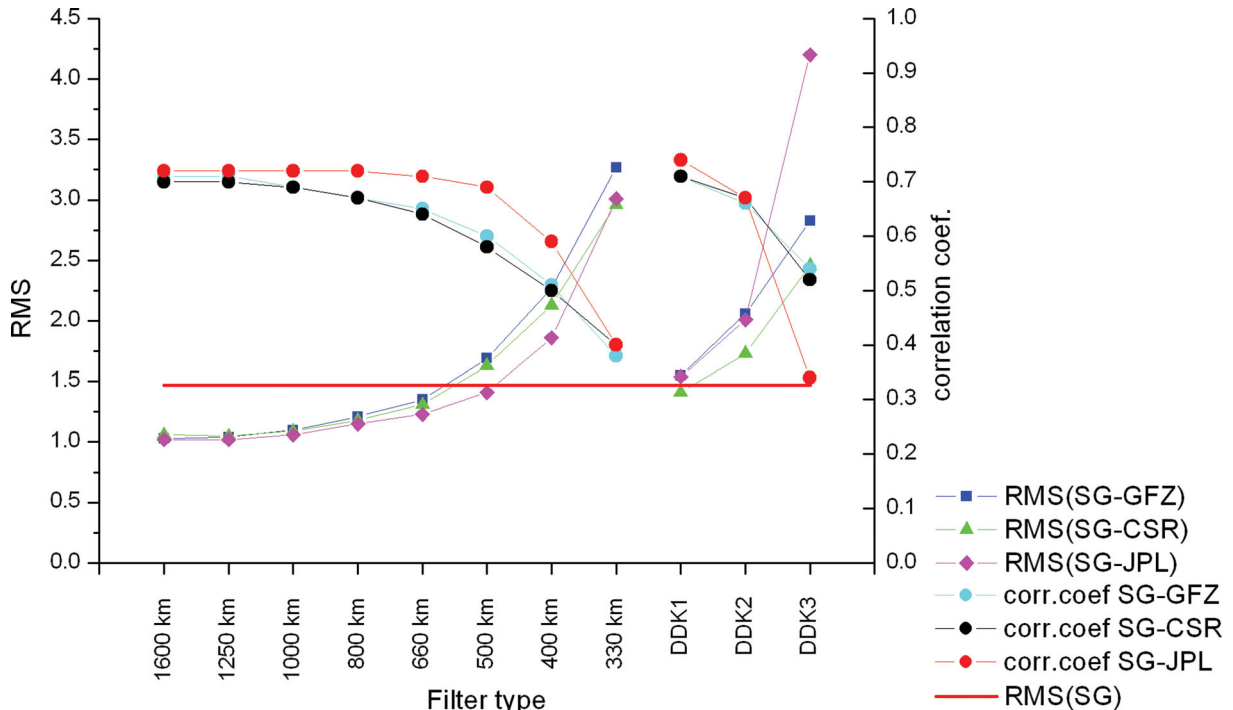


Figure 4. Overall rms of data set differences in micro-Gal and overall correlation coefficients between SG and GRACE gravity variations (different processing centres, details see text) with different filter types.

was used in this study. It considers water storage changes of snow, of unsaturated soil layers including saprolite down to 13 m depth and of groundwater. The model uses hourly precipitation, reference evapotranspiration and snow height as its inputs. The model parameters were calibrated using the Monte Carlo procedure and represent the interaction between atmosphere and soil. This procedure was also used for controlling the water storage in soil, saprolite and groundwater. Local hydrological measurements (soil moisture and groundwater) as well as the residual gravity variations were used as performance indices. In general, it can be assumed that local water storage changes are at least partly coherent with regional changes due to similar physiographic and climate conditions and weather patterns. Thus, the comprehensive local hydrological model removes part of the regional hydrological variations from the SG observations that are observed by GRACE. This is the reason why we found a different tendency for the rms values for WE between SG and GRACE data sets: While Neumeier *et al.* (2008) give an rms value of 2.35 for WE, we found a value of 1.91 (see Table 2). This decrease of the SG rms value for WE supports our hypotheses. That means that the separation of local from regional and global hydrological effects should be taken into account very carefully, as already noted in Neumeier *et al.* (2008).

On the other hand, Neumeier *et al.* (2008) have derived a correlation coefficient of -0.09 for the MO station. In our study, a correlation coefficient of 0.85 is found. This improvement is only a result of the more sophisticated local hydrological model available at this location (Naujoks *et al.* 2010), which we applied to the gravity data. In Neumeier *et al.* (2008) no local hydrological reduction was considered at the MO station.

Summarizing, it is found that applying a Gaussian filter with a length between 800 and 1600 km to the GRACE data delivers good agreement between GRACE- and SG-derived gravity variations. Based on these findings, we are searching for common characteristics between the SG and the GRACE data for the area of central Europe.

4 COMMON CHARACTERISTICS OF TIME-VARIABLE GRAVITY AT THE INCLUDED SG STATIONS

In this study the conventional EOF analysis based on the covariance matrix was used. Detailed explanations can be found, for example, in Preisendorfer (1988) or Wilks (1995). For the calculations the FORTRAN software distributed by David W. Pierce (Scripps Institution of Oceanography) (Pierce 2010) was used.

The EOF analysis has been applied separately to the SG residuals and the GRACE-derived variations. This means that each input file consisted of 36 monthly values from 2004 January to 2006 December for each of the six SG stations (i.e. 216 values per one input file). Based on the results from the correlation coefficients and the rms values (Section 3.2), only GRACE data smoothed with a Gaussian filter of 1000 km filter length were taken into account here.

First we checked how many EOF modes contain significant contributions to the signal. Fig. 5 shows the signal fractions (in per cent) for the modes 1–3 for the SG and GRACE time-series of GFZ, CSR and JPL.

Mode 1 as obtained from the SG time-series for six stations contains 70 per cent of the signal content of the monthly data. In the case of the GRACE data, mode 1 contains more than 90 per cent of the full data content (including signal and noise). The

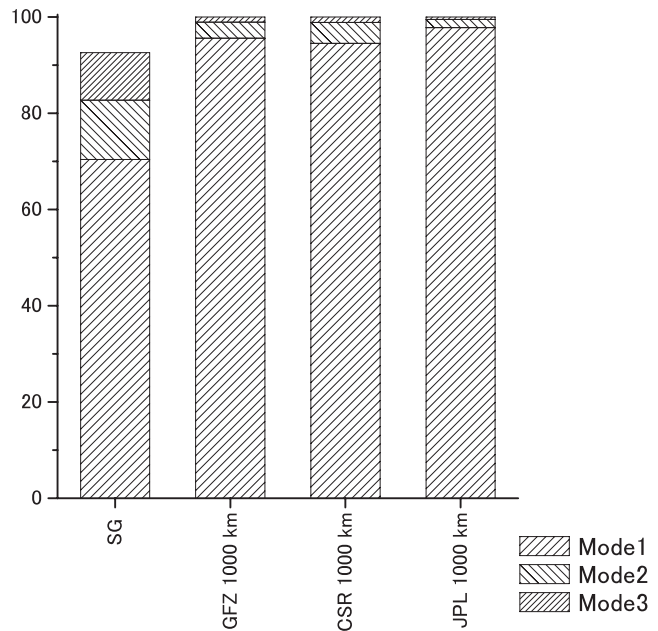


Figure 5. Signal fractions (in percentage) for the EOF modes 1–3 derived from EOF analyses, using SG monthly averaged data and GRACE data from different processing centres, filtered with a Gaussian filter length of 1000 km for six SG stations from 2004 to 2006.

EOF modes 2 and 3 for the SG stations still contain 12 and 10 per cent, respectively, of the total data content for the six SG stations (Fig. 5).

Since mode 1 for the GRACE solutions, and modes 1–3 for the SG observations, contain more than 90 per cent of the total signal content (including noise), we focus on these first three modes.

The results for the eigenvectors are shown in Fig. 6, as well as the related principal components for modes 1–3 of the SG data, and mode 1 of the GRACE data.

It is obvious from a comparison of the eigenvectors of mode 1 (Fig. 6a) that the eigenvector components obtained from the SG data show significantly larger values for WE than those found for GRACE. The WE component is highest (Fig. 6a) in the mode 2 eigenvector, and the corresponding values for the other stations are negative. This means that mode 2 of the SG residual for WE has reverse variation with respect to the other SG stations. The eigenvector of the SG EOF mode 3 contains variations which are anticorrelated between VI, WE and BH on the one hand and ST, MC and MO on the other hand (Fig. 6a). The SG mode 3 shows similar tendencies with a value of around 0.5 for MC and ST, -0.6 for VI and -0.2 for WE. The values for MO and BH are around zero (Fig. 6a).

Represented in Fig. 6(b), is the appearance of EOF mode 1 of the different GRACE solutions, in terms of variation of the principal components obtained from our EOF analysis. In the next step, the signals of mode 1 have been computed by multiplying the principal component with the corresponding component of the eigenvector associated with each station.

Fig. 7 allows a comparison between the SG data and the three GRACE solutions after applying a Gaussian filter of 1000 km filter length and, respectively, (a) the monthly original gravity variations for the six SG stations and (b) the signals of mode 1 for the six stations. The obtained rms values of mode 1 for each data type and station are shown in Table 3.

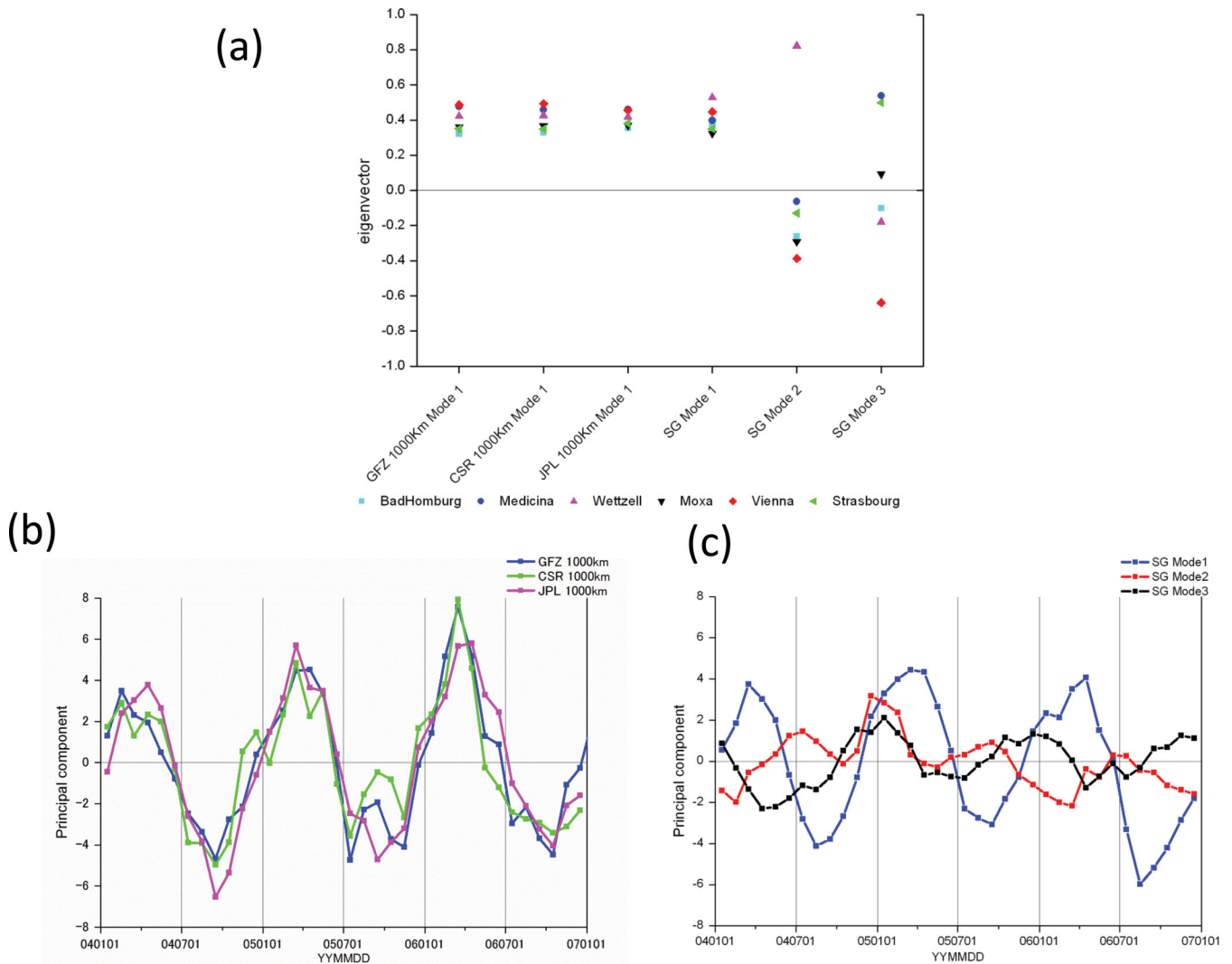


Figure 6. Eigenvectors of mode 1 for GRACE gravity field solutions from GFZ, CSR and JPL, filtered with a Gaussian filter length of 1000 km and modes 1–3 for SG at six SG stations: (a) associated principal component for GRACE EOF mode 1 and (b) associated principal components for SG EOF modes 1–3.

It is evident that the four types of time variations in mode 1, Fig. 7(b) fit better together than those in Fig. 7(a).

The largest rms values for mode 1 (Table 3) are found at (1) the WE station with a value of 1.62 μGal for the SG data, (2) the VI station for the GRACE solutions provided by GFZ (value of 1.54 μGal) and CSR (1.48 μGal) and (3) at the MC station for the JPL solution (1.54 μGal).

To estimate the size of the discrepancies between the signals of EOF mode 1, the rms values for the time-series of the differences [rms(diff)], and the correlation coefficients between the signals of mode 1 for the GRACE solutions, are given in Table 4(a). Those for the SG and the GRACE solutions are shown in Table 4(b).

In Fig. 7(b), discrepancies between the signals of mode 1 for the GRACE solutions are not that pronounced, however, the rms(diff) between the mode 1 signals of GRACE solutions (Table 4a) reaches around 40 per cent (relative to rms values for GRACE solutions). Nevertheless, these values are around 10 per cent smaller than the rms(diff) values obtained for the original monthly GRACE-derived gravity variations. The correlation coefficients between the signals of EOF mode 1 of the GRACE solutions are almost identical to the values obtained for the total monthly signals.

The correlation coefficients for EOF mode 1 between SG and GRACE solutions (Gaussian filter length of 1000 km) are all around the same value of 0.86 ± 0.02 (Table 4b). This is in contrast to the corresponding values for the original full signals (Fig. 4) of 0.69 ± 0.03 . Additionally, the rms(diff) values between the mode 1 signals reach 40–60 per cent, relative to the rms values of the full time-series (Table 4b). These rates are 20–40 per cent smaller than those of the differences between the full signals [e.g. in the case of the original time-series for a Gaussian filter length of 1000 km, the rms(diff) values vary from 40 to 102 per cent, relative to the rms values of full signals]. The signals of mode 1 between the SG and the GRACE time-series fit better together than the original monthly variations. This means that the first EOF mode reflects large-scale gravity signals that are seen both by GRACE and the SGs.

The SG EOF modes 2 and 3 of the SG data contain about 20 per cent of the complete gravity variations (Fig. 5). The most general signal content for all included stations has been decomposed to mode 1. It is of interest however, what kind of signals are remaining in modes 2 and 3 (Fig. 8).

Fig. 8(a) shows that the EOF mode 2 contains a strong signal at WE, which is particularly obvious at the beginning of 2005 and

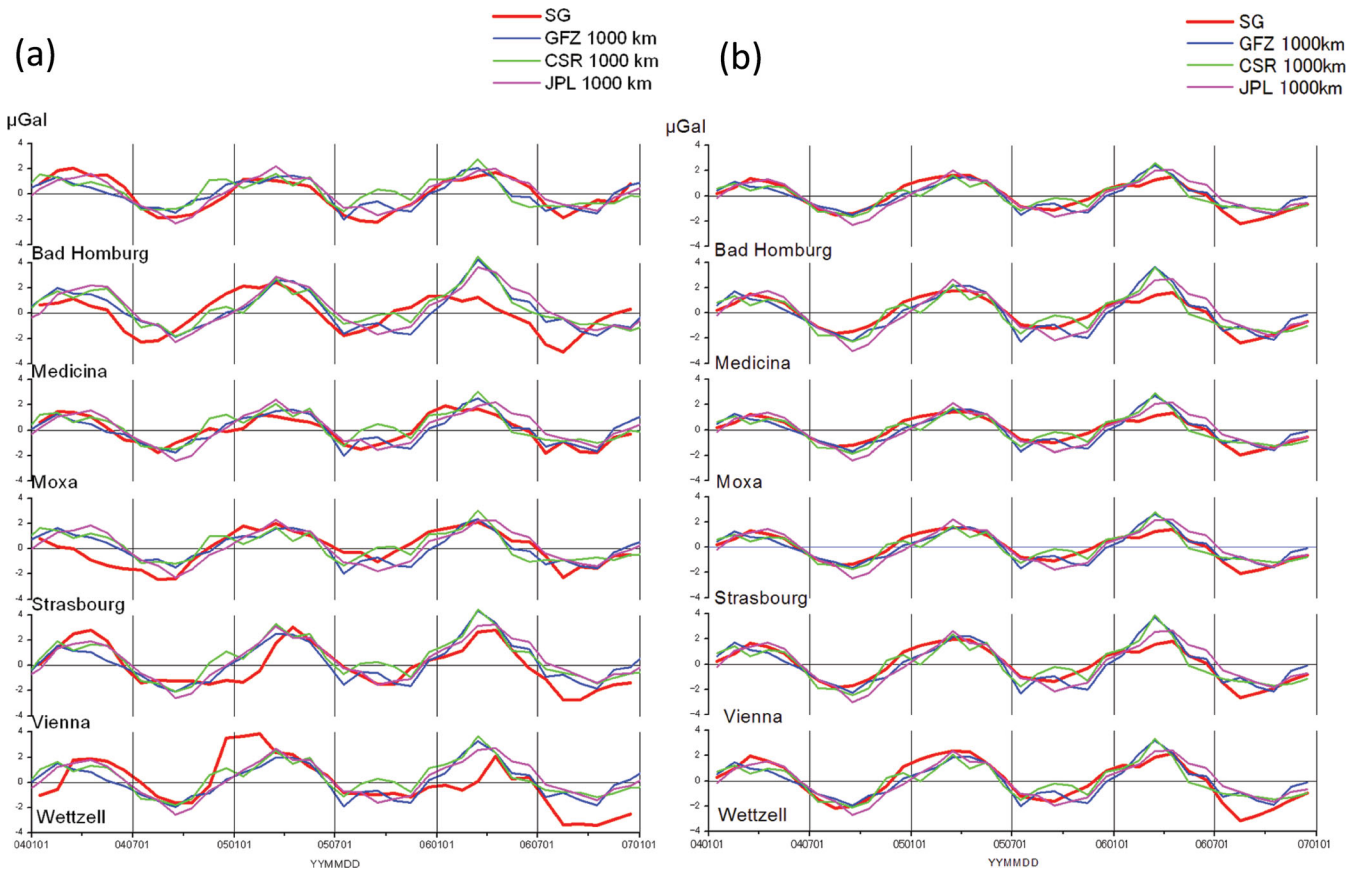


Figure 7. Comparison of SG with GRACE gravity variations of EOF mode 1 signals, and original monthly variations from the six European SG stations: the GRACE data are based on the GFZ, CSR and JPL solutions after applying a Gaussian filter of 1000 km length, for the years 2004–2006: (a) monthly original variations and (b) signals of the first mode derived from the EOF analysis.

Table 3. rms and overall rms (in μGal) of EOF mode 1, of the SG data for the six stations and GRACE-based gravity variations with a Gaussian filtering of 1000 km applied.

		Bad Homburg rms (μGal)	Medicina rms (μGal)	Moxa rms (μGal)	Strasbourg rms (μGal)	Vienna rms (μGal)	Wettzell rms (μGal)	Overall rms (μGal)
Mode 1	SG	1.13	1.21	0.99	1.07	1.37	1.62	1.25
	GFZ 1000 km	1.02	1.51	1.14	1.11	1.54	1.34	1.29
	CSR 1000 km	0.99	1.37	1.10	1.04	1.48	1.27	1.22
	JPL 1000 km	1.18	1.54	1.23	1.27	1.53	1.39	1.37

Table 4. rms of signal differences in μGal and the correlation coefficients between the EOF modes 1 of (a) the GRACE solutions after applying the Gaussian filter of 1000 km length and of (b) the SG and the GRACE solutions after applying a Gaussian filter of 1000 km length. The last two columns contain the overall rms(diff) and the correlation coefficients.

(a)	Bad Homburg rms(diff) μGal	Medicina rms(diff) μGal	Moxa rms(diff) μGal	Strasbourg rms(diff) μGal	Vienna rms(diff) μGal	Wettzell rms(diff) μGal	Overall rms(diff) μGal	Corr. coef.
GFZ-CSR 1000 km	0.43	0.63	0.48	0.46	0.65	0.56	0.54	0.91
GFZ-JPL 1000 km	0.47	0.62	0.49	0.51	0.62	0.56	0.55	0.92
CSR-JPL 1000 km	0.60	0.79	0.63	0.65	0.79	0.71	0.70	0.86
(b)								
SG-GFZ 1000 km	0.58	0.79	0.59	0.58	0.80	0.83	0.70	0.86
SG-CSR 1000 km	0.59	0.73	0.59	0.58	0.79	0.85	0.70	0.85
SG-JPL 1000 km	0.57	0.76	0.60	0.61	0.73	0.76	0.68	0.88

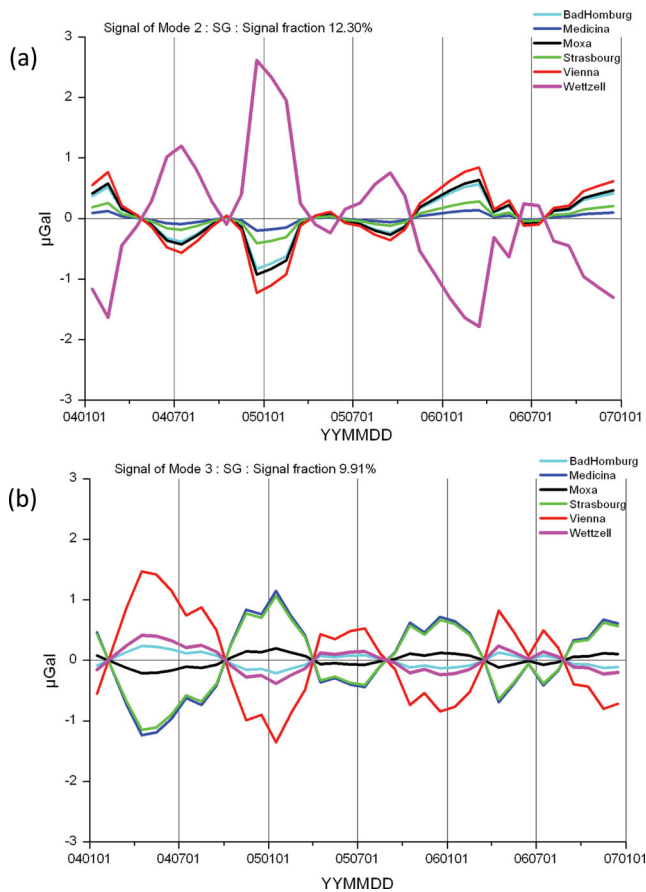


Figure 8. (a) Signals of the SG EOF mode 2 for the six SG stations. (b) Signals of the SG EOF mode 3 for the six SG stations.

around 2006 March. The appearance of this signal correlates with exceptionally heavy snowfall during this period, which was probably not completely modelled. Compared with other components of this eigenvector, the one belonging to WE is significantly high (0.82).

The conclusion is that the EOF mode 1 represents the European large-scale time-variable gravity signal, and the main station-specific variations deviating from mode 1 are decomposed into modes 2 and 3. It is of interest what factors are related to the SG EOF modes 2 and 3. Thus, further investigation should be done using EOF analysis applied to additional data sets, for instance soil moisture data (water storage) from hydrological models.

5 CONCLUSIONS

To evaluate the GRACE solutions by using terrestrial SG observations, we first compared GRACE solutions of different processing centres with two types of filters of different lengths, respectively, strengths. Overall rms values for monthly variations and for time-series of differences between GRACE solutions, as well as overall correlation coefficients, have been considered. As expected, the signal and noise power for the GRACE solutions increases when the filter length is shorter. The rms values for time-series of differences between GRACE solutions reach around 60 per cent of the rms values of the original variations. These discrepancies within the GRACE solutions are larger than expected. Since the main fea-

tures in the GRACE-derived time-series are similar, the correlation coefficients between different GRACE solutions are around 0.8.

The non-isotropic filter with the strongest filter effect (DDK1) results in a power of the same order of magnitude as obtained with Gaussian filters between 500 and 660 km in length.

For a cluster of six European SG stations, comparisons of terrestrial SG gravity variations with the GRACE-derived gravity changes, show that these changes are in general comparable with the terrestrial gravity variations. This has been already shown in previous studies. Comparisons of overall rms values and overall correlation coefficients between SG and GRACE data show that the highest correspondence is obtained when using an isotropic Gaussian filter with lengths between 800 and 1600 km.

An EOF analysis has been used to discover dominant and common signals in the gravity data sets. This investigation shows clearly that the dominant signal for the cluster of six SG stations can be separated out from the original monthly variations. Higher modes are also separated, and these may contain regional and remaining station-specific signals. This conclusion is based on results from the comparison of rms(diff) and correlation coefficients between original monthly data and the signals of EOF mode 1. However, there are still differences of up to 40 per cent between the mode 1 signals in the GRACE solutions (Gaussian filter length of 1000 km). Furthermore, the rms of differences between the SG and the GRACE solutions are between 40 and 60 per cent with respect to the rms of SG.

For future investigations, additional GRACE solutions should also be evaluated, for example, those provided by the Bonn University (Mayer-Gürr 2007), by GRGS/CNES (Bruinsma *et al.* 2009) and by the NASA/GSFC team (Luthcke *et al.* 2006b). Additionally, the investigated area should be extended to include other regions (e.g. southern hemisphere). Concerning the EOF results, further research is necessary. For instance, it would be interesting to look for geophysical interpretations of the signal content in SG modes 2 and 3. Clarification would come from finding a similar pattern as seen in SG modes 2 and 3, from EOF analysis applied to additional data sets (e.g. soil moisture data or water storage models).

ACKNOWLEDGMENTS

The authors thank the operators of the SG stations (ST and VI) for providing the data from their instruments. We are grateful to three reviewers for their useful comments also. This research was supported by the German Research Foundation in the frame of the priority programme SPP 1257 ‘Mass Transport and Mass Distribution in the Earth System’ (NE1409/1-1, KR 1906/13-2 IH 19/4-1, JE107/55-2, GU987/1-2), which is gratefully acknowledged. We are grateful to David W. Pierce for providing his EOF software.

REFERENCES

- Abe, M., Kroner, C., Neumeyer, J. & Chen, X.D., 2010. Assessment of atmospheric reductions for terrestrial gravity observations, *Bull. d' Inf. Météor. Climatol.*, **146**, 11 817–11 838.
- Bettadpur, S., 2007. UTCSR level-2 processing standards document for level-2 product release 0004 (CSR-GR-03-03), available at <http://isdc.gfz-potsdam.de/index.php?name=UpDownDownload&req=getit&lid=405> (last accessed 2012 September 3).
- Bruinsma, S., Lemoine, J.M., Biancale, R. & Vales, N., 2009. CNES/GRGS 10-day gravity field models (release 2) and their evaluation, *Adv. Space Res.*, **45**, 587–601.
- Creutzfeldt, B., Güntner, A., Klügel, T. & Wziontek, H., 2008. Simulating the influence of water storage changes on the superconducting

- gravimeter of the Geodetic Observatory Wettzell, Germany, *Geophysics*, **73**, WA95–WA104, doi:10.1190/1.2992508.
- Creutzfeldt, B., Güntner, A., Vorogushyn, S. & Merz, B., 2010a. The benefits of gravimeter observations for modelling water storage changes at the field scale, *Hydrol. Earth Syst. Sci.*, **14**, 1715–1730.
- Creutzfeldt, B., Güntner, A., Wziontek, H. & Merz, B., 2010b. Reducing local hydrology from high precision gravity measurements: a lysimeter-based approach, *Geophys. J. Int.*, **183**, 178–187.
- Crossley, D. & Hinderer, J., 2002. GGP ground truth for satellite missions, *Bull. d' Inf. Marées Terrestres*, **136**, 10 735–10 742.
- Crossley, D. et al., 1999. Network of superconducting gravimeters benefits a number of disciplines, *EOS, Trans. Am. Geophys. Un.*, **80**(11), 125–126.
- Crossley, D., Hinderer, J. & Boy, J.P., 2004. Regional gravity variations in Europe from superconducting gravimeters, *J. Geodyn.*, **38**, 325–342.
- Crossley, D., de Linage, C., Boy, J.P., Hinderer, J. & Chang, J., 2009. Validation of GRACE data using GGP stations from Europe and Asia, *Bull. d' Inf. Marées Terr.*, **145**, 11 741–11 750.
- Dehant, V., Defraigne, P. & Wahr, J.M., 1999. Tides for a convective Earth, *J. geophys. Res.*, **104**, 1035–1058.
- Farrell, W.E., 1972. Deformation of the Earth by surface loads, *Rev. geophys. Space Phys.*, **10**, 761–797.
- Flechtner, F., 2007. GFZ level-2 processing standards document for level-2 product release 0004 (GR-GFZ-STD-001), available at: <http://isdc.gfz-potsdam.de/index.php?name=UpDownload&req=getit&lid=401> (last accessed 2012 September 3).
- Flechtner, F., Dahle, C., Neumayer, K.H., König, R. & Förste, C., 2010. The release 04 CHAMP and GRACE EIGEN gravity models, in *System Earth via Geodetic-Geophysical Space Techniques*, 41–58, eds Flechtner et al., Springer-Verlag, Berlin, doi:10.1007/978-3-642-10228-8_4.
- Han, S.C., Shum, C.K. & Matsumoto, K., 2005. GRACE observations of M2 and S2 ocean tides underneath the Filchner-Ronne and Larsen ice shelves, Antarctica, *Geophys. Res. Lett.*, **32**, L20311, doi:10.1029/2005GL024296.
- Hinderer, J., Andersen, O., Lemoine, F., Crossley, D. & Boy, J.P., 2006. Seasonal changes in the European gravity field from GRACE: a comparison with superconducting gravimeters and hydrology model predictions, *J. Geodyn.*, **41**(1–3), 59–68.
- Hinderer, J., Crossley, D. & Warburton, R.J., 2007. Gravimetric methods: superconducting gravity meters, in *Treatise on Geophysics*, Vol. 3, pp. 65–122, ed. Herring, T.A., Elsevier, New York, NY.
- Hokkanen, T., Korhonen, K. & Virtanen, H., 2006. Hydrogeological effects on superconducting gravimeter measurements at Metsähovi in Finland, *J. Environ. Eng. Geophys.*, **11**, 261–267.
- Jekeli, C., 1981. Alternative methods to smooth the Earth's gravity field, Tech. Rep., 327, Ohio State University, Columbus, OH.
- Klügel, T. & Wziontek, H., 2009. Correcting gravimeters and tiltmeters for atmospheric mass attraction using operational weather models, *J. Geodyn.*, **48**(3–5), 204–210, doi:10.1016/j.jog.2009.09.010.
- Kurtenbach, E., Mayer-Gürr, T. & Eicker, A., 2009. Deriving daily snapshots of the Earth's gravity field from GRACE L1B data using Kalman filtering, *Geophys. Res. Lett.*, **36**, L17102, doi:10.1029/2009GL039564.
- Kusche, J., 2007. Approximate decorrelation and non-isotropic smoothing of time-variable GRACE-type gravity field models, *J. Geodyn.*, **81**, 733–749.
- Kusche, J., Schmidt, R., Petrovic, S. & Rietbroek, R., 2009. Decorrelated GRACE time-variable gravity solutions by GFZ, and their validation using a hydrological model, *J. Geodyn.*, **83**, 903–913.
- Lemoine, J.M., Bruinsma, S., Loyer, S., Biancale, R., Marty, J.C., Perosanz, F. & Balmino, G., 2007. Temporal gravity field models inferred from GRACE data, *Adv. Space Res.*, **39**, 1620–1629.
- Luthcke, S.B. et al., 2006a. Recent Greenland ice mass loss by drainage system from satellite gravity observations, *Science*, **314**, 1286–1289.
- Luthcke, S.B., Rowlands, D.D., Lemoine, F.G., Klosko, S.M., Chinn, D.S. & McCarthy, J.J., 2006b. Monthly spherical harmonic gravity field solutions determined from GRACE inter-satellite range-rate data alone, *Geophys. Res. Lett.*, **33**, L02402, doi:10.1029/2005GL024846.
- Lyard, F., Lefevre, F., Letellier, T. & Francis, O., 2006. Modelling the global ocean tides: a modern insight from FES2004, *Ocean Dyn.*, **56**, 394–415.
- Mayer-Gürr, T., 2007. ITG-Grace03s: the latest GRACE gravity field solution computed in Bonn, in *Grace Science Team Meeting and SPP Symposium*, 2007 October 15–17, Potsdam. [Available at <http://www.igg.uni-bonn.de/apmg/index.php?id=itg-grace03>.]
- Naujoks, M., Kroner, C., Weise, A., Jahr, T., Krause, P. & Eisner, S., 2010. Evaluating local hydrological modelling by temporal gravity observations and a gravimetric three-dimensional model, *Geophys. J. Int.*, **182**(1), 233–249, doi:10.1111/j.1365-246X.2010.04615.x.
- Neumeyer, J., Hagedoorn, J., Leitloff, J. & Schmidt, T., 2004. Gravity reduction with three-dimensional atmospheric pressure data for precise ground gravity measurements, *J. Geodyn.*, **38**, 437–450.
- Neumeyer, J., Schmidt, T. & Stöber, C., 2006a. Improved determination of the atmospheric attraction with 3D air pressure density data and its reduction on ground gravity measurements, *LAG Symp.*, **130**, 541–548.
- Neumeyer, J. et al., 2006b. Combination of temporal gravity variations resulting from superconducting gravimeter (SG) recordings, GRACE satellite observations and hydrology models, *J. Geodyn.*, **79**, 573–585.
- Neumeyer, J., Barthelmes, F., Kroner, C., Petrovic, S., Schmidt, R., Virtanen, H. & Wilmes, H., 2008. Analysis of gravity field variations derived from superconducting gravimeter recordings, GRACE satellite and hydrological models at selected European sites, *Earth Planets Space*, **60**(5), 505–518.
- Pierce, D.W., 2010. Empirical orthogonal function (EOF) software, principal component analysis (PCA) software, available at <http://meteora.ucsd.edu/~pierce/eof/eofs.html> (last accessed 2012 September 3).
- Preisendorfer, R.W., 1988. *Principal Component Analysis in Meteorology and Oceanography*, ed. Mobley, C.D., Elsevier Science Publishers, Amsterdam.
- Tamisiea, M.E., Mitrovica, J.X. & Davis, J.L., 2007. GRACE gravity data constrain ancient ice geometries and continental dynamics over Laurentia, *Science*, **316**, 881–883.
- Tamura, Y., 1987. A harmonic development of the tide generating potential, *Bull. Inf. Marées Terrestres*, **99**, 6813–6855.
- Tapley, B.D. & Reigber, C., 2001. The GRACE mission: status and future plans, *EOS, Trans. Am. geophys. Un.*, **82**(47), Fall Meet. Suppl., Abstract G41C-02.
- Velicogna, I. & Wahr, J., 2006. Measurements of time-variable gravity show mass loss in Antarctica, *Science*, **311**, 1754–1756.
- Wahr, J., 1985. Deformation induced by polar motion, *J. geophys. Res.*, **90**(B11), 9363–9368.
- Wahr, J., Molenaar, M. & Bryan, F., 1998. Time variability of the Earth's gravity field: hydrological and oceanic effects and their possible detection using GRACE, *J. geophys. Res.*, **103**, 30 205–30 230.
- Watkins, M. & Yuan, D.N., 2007. JPL level-2 processing standards document for level-2 product release 0004, available at <http://isdc.gfz-potsdam.de/index.php?name=UpDownload&req=getit&lid=400>.
- Weise, A., Kroner, C., Abe, M., Ihde, J., Jentzsch, G., Naujoks, M., Wilmes, H. & Wziontek, H., 2009. Terrestrial gravity observations with superconducting gravimeters for validation of satellite-derived (GRACE) gravity variations, *J. Geodyn.*, **48**, 325–330, doi:10.1016/j.jog.2009.09.034.
- Weise, A. et al., 2011. Tackling mass redistribution phenomena by time-dependent GRACE- and terrestrial gravity observations, *J. Geodyn.*, **59–60**, 82–91, doi:10.1016/j.jog.2011.11.003.
- Wenzel, H.-G., 1996. The nanogal software: Earth tide data processing package ETERNA 3.30, *Bull. d' Inf. Marées Terrestres*, **124**, 9425–9439.
- Wilks, D.S., 1995. *Statistical Methods in the Atmosphere Sciences: An Introduction*, Academic Press, San Diego, CA.
- Wziontek, H., Wilmes, H., Wolf, P., Werth, S. & Güntner, A., 2009. Time series of superconducting gravimeters and water storage variations from the global hydrology model WGHM, *J. Geodyn.*, **48**(3–5), 166–171, doi:10.1016/j.jog.2009.09.036.